LAWRENCE
LIVERMORE
NATIONAL
LABORATORY

UCRL-CONF-222314

Kinetic Modeling of Slow Energy Release in Non-Ideal Carbon Rich Explosives

P. Vitello, L. Fried, K. Glaesemann, C. Souers

June 21, 2006

13th International Detonation Symposium 2006
Norfolk, VA, United States
July 23, 2006 through July 28, 2006

Kinetic Modeling of Slow Energy Release in Non-Ideal Carbon Rich Explosives

P. Vitello, L. Fried, K. Glaesemann and C. Souers

Energetic Materials Center
Lawrence Livermore National Laboratory, Livermore, CA, 94550, USA

Abstract. We present here the first self-consistent kinetic based model for long time-scale energy release in detonation waves in the non-ideal explosive LX-17. Non-ideal, insensitive carbon rich explosives, such as those based on TATB, are believed to have significant late-time slow release in energy. One proposed source of this energy is diffusion-limited growth of carbon clusters. In this paper we consider the late-time energy release problem in detonation waves using the thermochemical code CHEETAH linked to a multi-dimensional ALE hydrodynamics model. The linked CHEETAH-ALE model treats slowly reacting chemical species using kinetic rate laws, with chemical equilibrium assumed for species coupled via fast time-scale reactions. In the model presented here we include separate rate equations for the transformation of the un-reacted explosive to product gases and for the growth of a small particulate form of condensed graphite to a large particulate form. The small particulate graphite is assumed to be in chemical equilibrium with the gaseous species allowing for coupling between the instantaneous thermodynamic state and the production of graphite clusters. For the explosive burn rate a pressure dependent rate law was used. Low pressure freezing of the gas species mass fractions was also included to account for regions where the kinetic coupling rates become longer than the hydrodynamic time-scales. The model rate parameters were calibrated using cylinder and rate-stick experimental data. Excellent long time agreement and size effect results were achieved.

INTRODUCTION

Detonation of a non-ideal, insensitive energetic material is a complex process involving coupled chemical kinetics and hydrodynamics. A numerical study of shock and detonation physics in high explosives involves unsteady compressible flow with shock waves, high-pressure equations of state (EOS), and modeling of the chemical kinetics for the reaction processes. While detailed chemical kinetics of detonations in homogeneous gases and liquids have been extensively studied, processes governing condensed solid insensitive energetic materials are much less understood. This is due to the higher densities, shorter reactive lengths and time scales, and more energetic nature of condensed detonations. For non-ideal explosives, such as those based on TATB, chemical reaction time scales can be comparable to the characteristic flow time scales leading to non-linear coupling between hydrodynamics and chemistry. Reaction rates in the dense fluid environment of a high explosive detonation are typically modeled using empirical reaction mechanisms due to the lack of knowledge of the exact physical processes that involve microstructure level phenomena[1-5].

For oxygen-deficient explosives composed primarily of C, H, N, and O (TATB has the chemical formula $C_6H_6N_6O_6$), carbon has the possibility of forming stable solid phase detonation products. All other products are gaseous. Solid carbon products may take intermediary form of graphite or diamond nano-clusters, liquid droplets or amorphous nano-particle coagulates (soot). Droplets freeze out before reaching the final product state, while other carbon products may survive. Interactions between the solid phase products and coagulation growth will tend to proceed much

more slowly than between gaseous products because clusters must diffuse spatially in order to react. The location of carbon phase equilibrium lines and other EOS properties can differ significantly from bulk materials because most atoms in small particles are located at or near the surface.[6] The slow growth of carbon particulates results in a long time scale energy release that should be considered self-consistently for accurate time dependent modeling.

To aid in studying the kinetics of energetic material detonations the CHEETAH[7] thermochemical code was coupled to a multi-dimensional Arbitrary Lagrangian Eulerian (ALE) hydrodynamic code. CHEETAH was used to determine the chemical properties of the reacting energetic material and to solve the chemical kinetic rate equations. CHEETAH using a high-pressure fluid equation of state determined the chemical composition of the reacting high explosive gases. The transformation of the high explosives into a reacting fluid of small product molecules was based on a simplified chemical kinetic rate scheme, whose coefficients were determined from fitting model results to measured detonation data. Non-rate controlled product species were assumed to be in thermodynamic equilibrium.

In this paper we present the first self-consistent kinetic based model for slow time-scale energy release in detonation waves in the non-ideal explosive LX-17 (92.5% TATB, 7.5% KEL-F). We model both the rate dependent burning of LX-17 and the growth of large graphite particulate clusters. These two rates when combined with pressure freezing of the equilibrium species allows for accurate time-scale coverage from microseconds to tens of microseconds behind the detonation front. Excellent agreement with experimental data is achieved.

MODELING OF CONDENSED EXPLOSIVES

Simulations of condensed (solid and liquid) explosives present numerous challenges. Kinetic reactions occur under extreme conditions, pressures up to 60 GPa and temperatures up to 4000 K. Equations of state for these regimes are complex and often very approximate. Explosive reaction mechanisms that have been developed[8-9] are appropriate for low-pressure gaseous kinetics only and are too detailed (involving up to 500 kinetic reactions between roughly 100 species) for current usage. High-density effects on the rates due to neighbouring atoms and molecules are poorly understood in these pressure and temperature regimes. Additionally, solid explosives are not always homogeneous like gases or liquids. For inhomogeneous non-ideal explosives, the initial phase of a detonation wave is believed to be dominated by the formation of "hot-spots"[3] which are localized regions of enhanced reactions formed at voids, grain boundaries and defects. Microstructure in the explosive and in the inert binder implies that any continuum model must represent highly averaged properties.

Adding to the physical complexity of high explosive processes is the experimental effort required in obtaining accurate data. The highly energetic reactions make data acquisition very difficult for large-scale explosive samples needed for non-ideal high explosive studies. These issues have made the application of detailed reaction mechanisms unfeasible. Modelling of high explosives has been primarily conducted using empirical models which specify the rate of transformation of the un-reacted explosive to its final product state. Typical models use equations of state estimated from experimental measurements such as the cylinder test and rate laws calibrated from shock initiation or cylinder size effect experiments.

General types of EOS models used for reactive flow calculations range from single fluid, two-state models to multi-fluid, two-state models. Simple single-phase, single-fluid models[1-5] consider the mixture of un-reacted and final product species as being represented by a single fluid with a separate effective EOS for each. Irreversible kinetics describes the evolution from pure un-reacted explosive to the completely burned product state. The EOS of the transient system of the mixture is only an estimate of its true value due to the lack of transient gas species or solid phases. More advanced single-fluid, two-phase models such as CHEETAH and CHEQ[10] track separate EOS contributions form multiple condensed phases and numerous individual gaseous species. These models have the ability to deal with detail non-equilibrium systems if the kinetic rates coupling the phases and species were known. Their estimates of the effective time varying EOS are based on a much more self-consistent model of the mixed state. The multi-fluid, two-phase model developed by Baer and Nunziato[11-12] treats the gas and solid phases as separate fluids with distinct densities, temperatures, and velocities. Kinetics is represented by a direct transformation from the un-reacted solid phase to the fully burned product gas. Thus the hydrodynamics is more accurately treated than for single-fluid models, but intermediate state effects are neglected

THE CHEETAH MODEL

CHEETAH is a numerical code that solves thermodynamic equations between chemical species to find their equilibrium state. It is assumed that a single gas phase composed of numerous species is in chemical equilibrium with possible multiple condensed phases each comprised of a single chemical species. Condensed phases may undergo solid-liquid phase transitions. A single temperature is assumed for all species. Thermodynamic equilibrium is found by minimizing the Gibbs free energy. While solving for the equilibrium state, CHEETAH guesses about the presence or absence of condensed species, then checks if these guesses are valid. Thermodynamic equilibrium results in pressure equilibrium between condensed and gas phases. For a fixed mass, the species molar concentrations, temperature, and density are the independent variables. The variables in CHEETAH must satisfy stoichiometric equations, balance of chemical potentials, and two thermodynamic conditions (such as a specified fixed energy and density). When applied to modeling the chemical kinetics of reactive flow, the species concentrations being treated through rate equations are held fixed while all other species concentrations are determined by minimizing the Gibbs free energy. The EOS for the gaseous species is based on an exponential-6 potential[13] for supercritical fluids, with a Murnaghan form[14] being used for solids and liquids. For the exponential-6 EOS, the parameters are chosen to reproduce shock Hugoniot and static compression data for a wide range of supercritical fluids[15]. This produces an accurate and complete EOS of the exponential-6 fluid based on HMSA integral equation theory and Monte Carlo calculations. Unlike previous detonation product sets, this model is not fit the EOS to detonation data.

In reactive flow modeling using CHEETAH the EOS typically treats 40-50 atomic, molecular, or condensed phase species. Specific species can explicitly be assumed not to form. This is done to speed convergence of the equilibrium calculation for species with negligible concentrations or to remove species that have formation time scales longer than any relevant modeling time. Multiple chemical reactions can be used to treat the detonation kinetics. These reactions can be considered irreversible or reversible reactions. For reversible reactions, CHEETAH calculates the reverse reaction automatically based on the forward reaction and the difference in the Gibbs free energy between initial and final species. Fast reactions are assumed to be in instantaneous equilibrium while slow reactions are treated directly. The assumption of instantaneous equilibrium for fast reactions removes the need of specifying complex unknown reactions that are not time resolved in the modeling. The ability to generate EOS data based on specific initial chemical composition and to treat continuous species states during burn calculations leads to flexibility in modeling multiple non-equilibrium processes such as aging effects in composite explosives.

In the CHEETAH/ALE chemically reacting flow model, the ALE code handles transport. Transport and chemical kinetics are time split. Calls are made by the ALE code to CHEETAH for EOS evaluations of the pressure, temperature and sound speed and for kinetic rate evaluations to update the species mass fractions. To update the species mass fractions the ALE code makes two rate calls to CHEETAH. The first takes a half time-step to obtain mid-step values. These mid-step values are then used by the ALE code to take a second order in time accurate full time-step. Internal to CHEETAH, the chemical kinetics is solved using an adjustable time step that sub-cycles within the fluid dynamic time step. CHEETAH allows the user to choose from several ordinary differential equation (ODE) solvers including efficient explicit 2nd and 4th order Runge-Kutta solvers and the high order implicit CVODE[16] ODE solver that can treat stiff kinetic rate equations. The time over which CHEETAH advances the species concentrations is determined by the ALE code. It is typically limited such that the largest change in species concentration is less than 20%. With this time step control, CHEETAH usually only takes one step in its internal ODE solver.

A key point of CHEETAH/ALE is the use of a multi-dimensional sparse hash table in place of the direct calculation of EOS data. For hydrodynamic calculations using tens of thousands to millions of spatial zones, table lookup and interpolation was found to be orders of magnitude faster than direct EOS evaluation, and a sparse table allows for a practical table size when multiple species are being treated.

Rate equations in CHEETAH can take many forms including:

- Pressure power-law

$$\frac{dX_i}{dt} = AX_i^B(1-X_i)^C P^D \qquad (1)$$

- Arrhenius

$$\frac{dX_i}{dt} = X_i X_j A T^B \exp\left(-\frac{E}{kT}\right) \quad (2)$$

- Complex CHEMKIN style (pressure, temperature) kinetic rate laws[17].

Reverse reactions can be calculated self-consistently from the non-ideal EOS data, enforcing equilibrium species concentrations at large times. In the pressure power-law rate model shown in eq. (1) the effective numerical pressure, which is the physical pressure P plus the numerical artificial viscosity Q, is generally used. As the effective pressure is what is used in the fluid momentum and energy equations, its use in the rate law allows for a more self-consistent treatment. Accuracy is also enhanced if P + Q is used for low spatial resolution where Q may contribute a significant fraction of the total force at the detonation shock front.

The rate models used currently in CHEETAH/ALE are simple phenomenological expressions meant to be used to explore the kinetics of detonation behaviour. The effective pressure power-law rate form was used in this paper for all kinetic modelling.

At low temperatures and pressures it is expected that the assumption of chemical equilibrium for non-rate controlled species breaks down. In this regime kinetic rate time scales become longer than hydrodynamic time scales and the chemical mass fraction values effectively "freeze" out and become constant in time. This is implemented in the CHEETAH/ALE code through a freeze pressure parameter. For pressures below the freeze pressure the non-rate controlled mass fractions are approximately frozen in time. A detailed self-consistent implementation of this behaviour in a hydrodynamics model would involve the spatial tracking of history variables that contain the condition at the time the freeze pressure was reached. We use an approximate freeze model with no history variables. The frozen mass fractions are calculated by taking values of energy, mass density, and rate controlled mass fractions below the freeze pressure, calculating their entropy, and then calculating the equilibrium species mass fractions at this entropy and at the freeze pressure value. The resulting mass fractions are close to those to the values resulting from adiabatic expansion after freezing and allow for re-mixing of products formed below the freeze pressure from the rates being explicitly treated.

SPARSE HASH TABLE

CHEETAH calculates dependent variables needed by the ALE model using Piecewise-Linear Interpolation (PLI) or Multivariate Polynomial Interpolation (MVPI) from either a 2D (ρ, E) table or from a sparse hash table. Unlike most table look up schemes, CHEETAH calculations do not require input of complete data tables, where data has been pre-calculated for all expected values of the independent variables. If not available, table entries needed for the interpolation scheme are generated by CHEETAH dynamically. Thus the sparse and 2D tables can be built efficiently on the fly during a hydrodynamic simulation. For parallel calculations, new table entries are periodically passed to all other processors to maintain synchronization of the tables. Parallel calculations where different processors are simultaneously treating different conditions for the detonation wave propagation can significantly speed the creation of the total data table. Since table data is written to a binary file as part of the standard simulation output, one can add to existing data tables by sequentially running simulations covering different regimes of the independent variables. To expand the table, each new case would use as input the final saved data table from the previous calculation. This use of pre-calculated sparse or 2D table data improves efficiency and stability, but is not necessary. As the detonation wave structure changes slowly as it propagates, the extra computational overhead for simulations done without the use of a pre-existing data table occurs predominantly during the early portion of a simulation.

The independent sparse table variables are (ρ, E, X_i), which correspond to density, energy per gram, and mass fractions of the N species that are to be evolved using kinetic laws. There are $N_s = N + 2$ independent variables. Table spacing is uniform in density (or log density), energy, and molar concentration. The dependent variables stored in the table are the pressure, temperature, thermodynamic partial derivatives, and mass fractions of species in instantaneous equilibrium.

In calculating dependent variables it is first determined whether a fast 2D table or a sparse hash table look up should be used. The 2D tables are only used for the un-reacted or fully reacted regions where the rate controlled species concentrations are fixed. 2D table lookup and interpolation is very much faster than for the

sparse table, but is limited in its applicability. Use of a sparse hash table was found to allow the strengths of CHEETAH to be applied to reactive flow modeling. Dense multi-dimensional tables become very large as the number of kinetic species increases. Such tables are memory intensive to use and expensive computationally to generate. Sparse tables generated from trial calculations tend to correspond to data on a hyper-surface. The sparse table basically only contains useful data points.

In 2D and 3D ALE calculations both the number of spatial grid points and the number of time-steps can be very large. It is therefore important to consider the amount of work needed to evaluate data from the table look up. The 2D table is only used during simple EOS calls. Two-dimensional linear interpolation is used for the 2D tables. The number of table evaluations needed per dependent variable is therefore four per EOS call. For the sparse hash table there are two interpolation schemes to choose from. The number of table lookups needed when using MVPI scales as (Interpolation Order)^{Ns} per EOS call and as (Interpolation Order)^{Ns} x (ODE Order) per rate call. The MVPI scheme makes use of a product of locally fitted polynomials whose coefficients are chosen such that the exact table data values are recovered. This is very accurate if phase discontinuities do not exist, but can be very computationally intensive even for first order linear interpolation as the number of independent variables N_s increases. For linear interpolation and two kinetic controlled species the number of table evaluations needed for interpolation is 2^4.

An alternative, faster interpolation scheme used by CHEETAH is PLI[18-19]. For a multi-dimensional table with uniform spacing in each dimension, PLI is an efficient, robust, continuous, first order scheme that corresponds to interpolation along the surface of the hypercube containing the point to be interpolated to. The hypercube is formed by the points i, i+1, j, j+1, k, k+1, …, which bracket the interpolation point. The interpolation path is determined by sorting in decreasing order dx_n, which are the distances in the various directions from the interpolation point to the table point (i, j, k, …). Each distance dx_n is scaled by the table grid spacing for its appropriate direction such that it varies from 0 to 1. The scheme starts by taking the starting table entry at (i, j, k, …), determining the dimension of the largest dx_n (say m), and adding dx_m times the difference between the starting table and the table entry with the mth dimension incremented by 1. The beginning of the interpolation path thus starts from the beginning table entry and takes a step in the mth direction. This is the beginning point for the next interpolation step. The dimension of the next largest dx_n is now determined and the linear interpolation in this dimension is added. Each dimension is treated in succession, with a step being taken along the hypercube. Linear interpolation is done for each step between points along this step. For PLI the number of table lookups needed scales as (N_s + 1) per EOS call and as (N_s + 1) x (ODE Order) per rate call. The PLI scheme requires a sort of length N_s that increases its operation count.

To illustrate the typical degree of sparsity in our modelling we consider there two treatments of a LX-17 5mm rate-stick i) a single rate model burning LX-17 to product gases and ii) a two rate scheme burning TATB and KEL-F separately to product gases. For simplicity we use the identical pressure squared dependent kinetic rate for all processes so the one rate and two rate cases give the same detonation. The rate coefficients A, C, and D for the cases are (0.049, 1.5, 2). The units of A are $\mu s^{-1} GPa^{-D}$. The PLI interpolation scheme is used with a second order Runga-Kutta difference scheme. We have used a moderately fine mesh that was initially 80 zones per cm. The rate-stick was impulse initiated by applying a velocity of 0.2 cm/μsec to an annulus containing the first three axial mesh points. This leads to an initial over driving of the detonation wave and avoids the need to model ignition in detail.

The cache generated by a steady state rate-stick region of the one rate flow is shown in Figure 1. The solid dot corresponds to unburned initial conditions. Sparse cache geometry reflects phase space evolution of spatial points in the hydrodynamic simulation. A given spatial point on the rate-stick follows a path in density, energy, and mass fraction phase space as it evolves in time. The higher order the interpolation scheme, the thicker the resulting data path generated. Except for spatial points near the rate-stick surface, the paths show initial compression and increased energy followed by near adiabatic expansion as the mass fraction drops. The final value for the mass fraction increases with increasing initial spatial radius position. This is a result of the decreasing detonation wave pressure with radius producing to a lower burn rate. Except near the rate-stick surface the hydrodynamic ALE mesh motion is Lagrangian and changes in the mass fraction are entirely due to burning of the explosive.

The near 2D nature of the detonation wave cache evident in Figure 1 was verified by decreasing the data spacing by a factor of two for the density, energy, and mass fraction. For a dense data table this would lead to a increase in the table size by a factor of 2^3. What was found was an increase of only a factor of 3.985. This is nearly equal to 4, which is the increase for an increase in resolution of a purely two-dimensional surface. Simulations using two rates were similarly found to have roughly two-dimensional surface cache structures. For the two rate case (which has 4 independent dimensions) decreasing the cache data spacing leads to a factor of 4.1 increase in the number of cache entries. Dense tables would respectively show a 16-fold modification. Further modeling with three rates and with a variety of different geometries has verified the hyper-surface nature of our sparse cache table for LX-17 detonations.

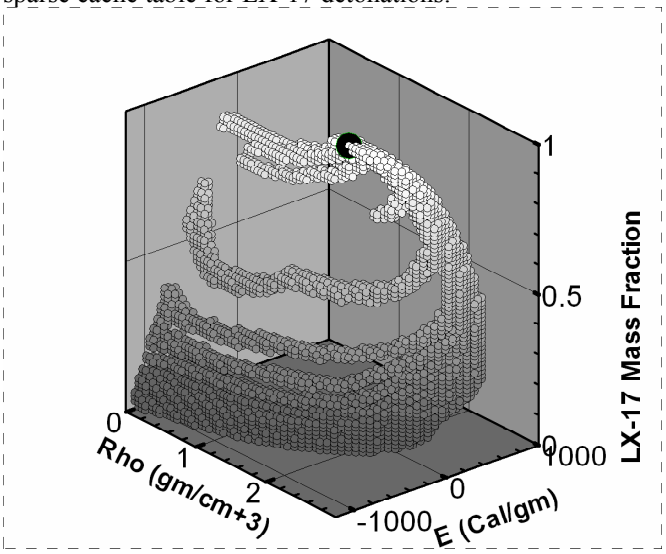

Figure 1. Sparse cache phase space.

CARBON

Free carbon appears when oxygen-deficient explosives detonate. These are materials with highly negative oxygen balances, OB, as defined by[20]

$$OB = \frac{1600\Delta O}{MW} \quad . \qquad (3)$$

In eq. (3) ΔO is the excess number of oxygen atoms (positive or negative) after assumed full reaction to CO_2, MW is the molecular weight of the initial explosive, 16 is the molecular weight of atomic oxygen, and the factor 100 is added to convert the results to percent. Because OB is defined in terms of full burn to CO_2, even PETN and HMX are negative. Dynamites and ANFO's are defined to be at zero values of OB.

Solid carbon comes in three forms: soot, graphite, and diamond. Soot is a thought to be made up of clusters of nanometer-sized particles of diamond, graphite, and amorphous carbon. Amorphous carbon usually appears to be partly a mixture of damaged graphite and maybe some diamond crystals with short-range but no long-range order. It also contains other elements, and it has distorted and dangling bonds and a higher energy than a crystalline form. Currently CHEETAH treats soot as being a form of graphite with a heat of formation chosen to reflect its higher energy.

In Table 1 we list data that we feel can be reasonably compare with CHEETAH calculations. Experimental data given in the table are the composition percentage for mixed explosives, the experimental mass, and the measured mass of all recovered carbon, all non-diamond carbon, and all diamond carbon. The calculated data are the OB values and the mol Carbon / mol Explosive. The calorimetry data is taken from samples that were contained and/or were fired into a gaseous atmosphere. Some diamond results were included as long as part of it agrees with the calorimetry. Other data contains calorimetry shots unconfined or in vacuum so that lower carbon yields were obtained. Finally, we list the diamond producing experiments where we think some enhancing process was used. Figure 2 shows the Table 1 data plotted as a function of oxygen balance. There is a clear correlation. The carbon value drops to zero at OB of ~10%, which is where PETN is. LX-17, which is the explosive considered in this paper should behave similar to TATB, with high carbon production.

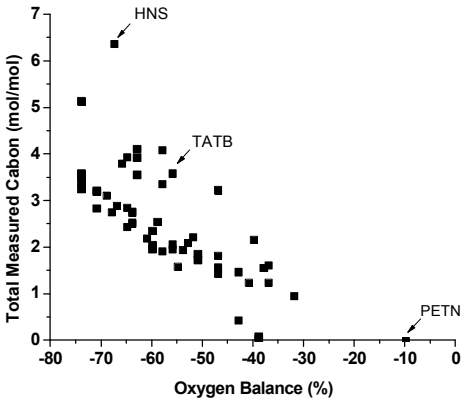

Figure 2. Total measured carbon produced as a function of OB.

Table 1. Summary of Carbon Data

% TNT	% HMX	Measured mass (g). Expl. mass	All C	ND	D	OB	mC / mE	ref
30	70	310	21.7	4.8	16.9	-47	1.58	22
30	70	315	20.2	8.4	11.8	-47	1.45	22
40	60	100	8.5	2.9	5.6	-51	1.87	23
40	60	320	25.3	4.9	20.4	-51	1.74	22
50	50	100	9.7	3.2	6.5	-56	2.07	23
50	50	320	29.4	6.4	23	-56	1.97	22
60	40	312	29.4	8.1	21.3	-60	1.97	22
60	40	100	11.4	4.4	7.0	-60	2.37	23
70	30	310	38.4	12.7	25.7	-64	2.52	22
70	30	298	37.3	12.8	24.5	-64	2.55	22
70	30	100	13.6	7.0	6.6	-64	2.76	23
80	20	100	14.6	9.3	5.3	-67	2.90	23
90	10	100	16.6	12.8	3.8	-71	3.21	23
90	10	288	42.4	30.5	11.9	-71	2.85	22
100	0	280	50.8	42.8	8	-74	3.43	22
100	0	100	18.8	16.4	2.4	-74	3.55	23
TNT	PETN							
35	65	100	5.4	2.0	3.4	-37	1.26	23
40	60	100	5.5	1.8	3.7	-41	1.26	23
50	50	100	8.3	3.6	4.7	-47	1.83	23
60	40	100	9.9	4.6	5.3	-53	2.11	23
70	30	100	12.4	6.7	5.7	-59	2.56	23
80	20	100	13.9	9.3	4.6	-64	2.78	23
90	10	100	16.0	12.7	3.3	-69	3.12	23
100	0	100	18.8	16.4	2.4	-74	3.55	23
TNT	RDX							
0	100	200	16.0	9.0	7.0	-43	1.48	25
35	65	250	21.6			-54	1.96	24
40	60	100	8.6	2.7	5.9	-55	1.60	23
50	50	200	36.0	17.8	18.2	-58	3.37	25
50	50	100	10.3	3.4	6.9	-58	1.92	23
55	45	100	11.0	3.6	7.4	-60	2.06	23
60	40	100	11.7	3.9	7.9	-61	2.20	23
65	35	200	38.0	29.0	9.0	-63	3.57	25
70	30	250	34.6			-65	2.86	24
70	30	200	42.0	39.8	2.2	-65	3.95	25
70	30	100	13.0	6.0	7.1	-65	2.45	23
80	20	100	14.7	8.5	6.2	-68	2.77	23
90	10	100	17.1	12.7	4.4	-71	3.23	23
100	0	100	18.8	16.4	2.4	-74	3.55	23
100	0	200	54.4	48.8	5.6	-74	5.15	23
50*	50	200	43.8	28.8	15.0	-58	4.10	25
65*	35	200	42.0	38.2	3.8	-63	3.94	25
65**	35	200	44.0	41.4	2.6	-63	4.13	25
NM	RDX							
40*	60	200	48.2	47.6	0.6	-40	2.17	25
NQ	RDX							
50*	50	200	17.4	16.6	0.8	-37	1.63	25
TNT	NQ							
50	50	305	36			-52	2.23	21
TNT	TATB							
50	50	301	57			-66	3.81	21

Calorimetry-Dense and Somewhat Confined	g/cc		OB	mC/ mE	
BTF	1.86		-38	1.57	26
FEFO	1.61		-10	0	26
HMX	1.89	confined	-32	0.97	26
HNS	1.65		-67.5	6.38	26
NM	1.13	ends closed	-39	0.095	26
NM	1.13	ends open	-39	0.045	26
PETN	1.74	all conditions	-10	0	26
RDX	1.76		-43	0.44	26
TATB	1.87		-56	3.6	26,27
TNT	1.53	ends closed	-74	3.6	26
TNT	1.53	ends open	-74	3.27	26

Quenched in * water; ** ice

The nanometer scale diamond particles recovered in detonation experiments are typically spherical in shape, suggesting that they must have formed in the liquid state.[6] Pressure-temperature hugoniots of explosives however do not approach the bulk diamond melting line until pressures are well above 100 GPa. As such pressures are well above typical explosives C-J pressures it is expected that lowering of the melting temperature must have occurred. This is expected, as bonding at the surface in nanometer scale particulates is different than in

the interior, and particles at this scale have a significant fraction of atoms with surface bonding as opposed to interior volume bonding. Viecelli et al.[6] suggest that the correction for surface energy for spherical particles can be approximated as

$$\delta E_n = \Delta E_0 n^{-1/3}, \qquad (4)$$

where δE_n is the average per atom difference in energy between carbon particles of n particles and bulk carbon. The parameter ΔE_0 is estimated to be for diamond, graphite, and liquid respectively as ~70 kcal/mol, ~40 kcal/mol, and ~1 kcal/mol. Liquid droplets freeze out before reaching the final product state, while other carbon products may survive. Interactions between the solid phase products and coagulation growth will tend to proceed much more slowly than between gaseous products because clusters must diffuse spatially in order to react.

In the model presented here we ignore the distinction between liquid, diamond, and graphite particulate formation for simplicity. Experimental data for LX-17 detonation is not sufficient to explore details of the liquid and diamond phase and their energy release effects. Instead we present a reactive flow rate model where all solid carbon is in the graphite phase. We treat the full range of graphite particles sizes using two representative values, small and large with respective heats of formation of 60 kcal/mol and 7.8 kcal/mol. Modeling results are weakly dependent upon the value of the heat of formation for the large graphite particles as long as it is much smaller than that of the small particles. The difference in particle energy of roughly 50 kcal/mol was found to give long time energy release consistent with experiments. The smaller particles are assumed to be in chemical equilibrium with the product gas, while larger particle production is rate controlled. Our rate model thus consists of two rates, a fast timescale pressure squared dependent burn rate for LX-17 to products and a slower temperature dependent Arrhenius rate for the transformation of small graphite particles to large graphite particles. Rate parameters were determined using small the scale experiments discussed below. For prompt detonation conditions where LX-17 is nearly totally burned, the fast LX-17 burn rate is on the order of microseconds, while the slower carbon rate is on the order of tens of microseconds. The experimental data considered allows only for over all time scale and energy release. Fine details such as diamond production and the distribution of carbon energy release between diamond and graphite formation are not considered.

LX-17 MODEL RESULTS

We consider here the effect of carbon particulate growth on slow timescale energy release for LX-17. Using the CHEETAH/ALE code we model the rapid burning of LX-17 using an effective pressure rate-law of the form given in eq. 1 with rate coefficients A, C, and D for the cases are (0.05, 1.5, 2). The units of A are μs^{-1} GPa^{-2}. The rate for large graphite particulate growth from small graphite particles is treated using the Arrhenius rate form in eq. 2, with parameters A, B, and E equal to (0.2, 0, 2000 K). The freeze pressure was set to 1.105×10^5 GPa. The rate parameters values were determined by comparisons with small-scale experimental data.

We first consider the detonation velocity variation as a function of radius for cylindrical rate sticks. Figure 3 shows that the calculated CHEETAH/ALE size effect variation from slightly larger than the failure diameter to large radii system. Agreement with experimental data[28] is very good at all radii. Calculated detonation velocities are weakly dependent on the carbon kinetic model and strongly dependent on the LX-17 burn rate. This is expected as the carbon energy release primarily occurs at late time outside of the reaction zone. This allowed us to determine our LX-17 rate essentially independent of the carbon rate.

Long time scale experimental data is needed to calibrate our carbon rate. For this we used fabry velocity measurements for a one-inch diameter cylinder of LX-17 that was confined by 2.6 mm thick copper. In Figure 4 we show results a comparison of modeling and the experimental data. The timing of the simulations was adjusted to align the curves at the steepest region after the initial jump. This is to account for possible timing error in the experimental data. The experiment fabry velocity measurements compare extremely well with our two-rate model velocity calculations. The two-rate model agrees at time scales from several to tens of microseconds. For comparison we show CHEETAH/ALE results for a one-rate model where large graphite is not rate controlled, but allowed to be in chemical equilibrium with the other product species. This results in too rapid an energy release behind the detonation front and poor agreement with data. As opposed to the size effect simulations, the cylinder calculation is very sensitive to the

carbon model and weakly dependent upon the LX-17 burn rate model. For this case long time scale effects dominate. As long as LX-17 is nearly completely burned in the reaction zone on a time scale of a few microseconds, then the absolute value of the LX-17 burn rate has little effect on the late time pressure which determines the velocity.

We found that freeze pressure adjustments about the chosen freeze pressure value affected the curvature of the velocity curve at times roughly 5 microseconds after the detonation front. Variations in the small to large graphite rate tend to mainly modify the velocity at later times, on the scale of 10-20 microseconds after the detonation front. Thus the two parameters could be separately adjusted to achieve the best agreement.

Using CHEETAH we are able to track the time dependent chemistry behind the detonation front. The on axis time history of the dominant chemical components is show in Figure 5. The thick curves correspond to solid phase species of LX-17, small particulate graphite (C_S) and large particulate graphite (C_L). The burning of LX-17 on a microsecond timescale is evident, as is the slower, tens of microsecond timescale C_S to C_L reaction. The effect of pressure freeze is evident at a time roughly 5 microseconds after the detonation front. The simulation predicts approximately 3 moles of solid carbon per mode of LX17 at 30 microseconds. This is in good agreement with the TATB experimental data results of 3.6 moles per mole given in Table 1.

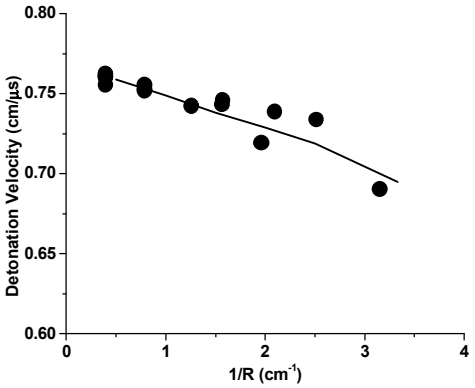

Figure 3. Size effect curve for LX-17. The solid curve shows model calculations. Dots correspond to experimental data.

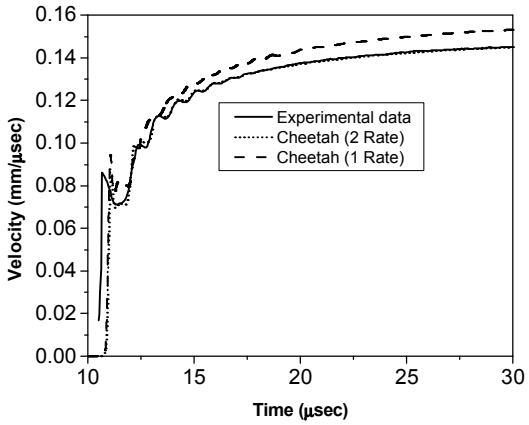

Figure 4. Surface velocity history for a one-inch diameter cylinder of LX-17 confined by 2.6 mm of copper.

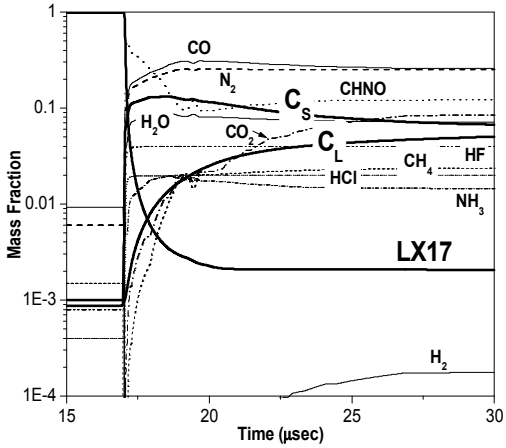

Figure 5. Chemical time history on axis for a one-inch diameter cylinder of LX-17 confined by 2.6 mm of copper.

CONCLUSIONS

The addition of a slow carbon energy release rate to LX-17 detonation our modeling has produced excellent agreement with experimental data from microsecond to tens of microsecond timescales. The CHEETAH/ALE model self-consistently treats product species behind the detonation front, producing highly accurate EOS values. This self-consistency is necessary to properly simulate confined systems where re-shocks play a significant role in kinetic energy delivery. The combination of detailed EOS and multiple time scale rates results in our detonation modeling having major

enhancements over previous models.

ACKNOWLEDGEMENTS

This work was performed under the auspices of the U.S. Department of Energy by the University of California Lawrence Livermore National Laboratory under contract No. W-7405-Eng-48.

REFERENCES

1. Lee, E. L. and Tarver, C. M., "Phenomenological Model of Shock Initiation in Heterogeneous Explosives," *Phys. Fluids*, Vol. 23, p. 2362, 1980.

2. Johnson, J. N., Tang, P. K., and Forest, C. A., "Shock-wave initiation of heterogeneous reactive shields," *J. Appl. Phys*., Vol. 57, p. 4323, 1985

3. J. Field, N. Bourne, S. Palmer, S. Walley, and J. Smallwood, "Hot-spot ignition mechanisms for explosives and propellants", *Phil. Trans. Roc. Soc. London Series A-Mathematical Physical and Engineering Sciences*, 339, 269, 1988.

4. Souers, P. C., Anderson, S., McGuire, E., and Vitello, P., "JWL++: A Simple Reactive Flow Code Package for Detonation," *Propellants, Explosives, Pyrotechnics*, Vol. 25, p. 54, 2000.

5. Leiper, G. A., Kirby, I. J., and Hackett, A., "Determination of Reaction Rates in Intermolecular Explosives Using The Electromagnetic Particle Velocity Gauge," *Proceedings Eigth Symposium (International) on Detonation*, Albuquerque, New Mexico, July 15-19, 1985, p. 185.

6. Viecelli, J. A., and Ree, F. H., "Carbon particle phase transformation kinetics in detonation waves," J. Appl. Phys., 88, p. 683, 2000.

7. Fried, L. and Howard, M., "Cheetah 3.0 Users Manual", Lawrence Livermore National Laboratory UCRL-MA-117541, 2001.

8. D. Chakraborty, R. Muller, S. Dasgupta, and W. Goddard, "The mechanism for unimolecular decomposition of rdx (1,3,5-trinitro-1,3,5-triazine), an ab ignition study," *J. Physical. Chem. A*, 104 2261, 2000.

9. K. Prasad, R. Yetter, and M Smooke, "An eigenvalue method for computing the burning rates of rdx propellants," *Combustion Sci. Tech*., 124, 35, 1997.

10. F.H. Ree, Viecelli, J.A., and Glosli, J.N., "Modeling the Kinetics of Carbon Coagulation in Explosives Detonation," *J. Computer-Aided Materials Design*, 5, 265, 1998.

11. Baer, M. and Nunziato, J. W., "A 2-phase mixture theory for the deflagration-to-detonation transition (ddt) in reactive granular materials," *Int. J. Multiphase Flow,* 12, 861-889, 1986.

12. Bdzil, J., Menikoff, R., Son, S., Kapila, A., and Stewart, D., "Two-phase modeling of deflagration-to-detonation transition in granular materials: A critical examination of modeling issues," *Phys. Fluids*, 11, 378-402, 1999.

13. Fried, L. E., and Howard, W. M., "An Accurate Equation of State for the Exponential-6 Fluid Applied to Dense Supercritical Nitrogen", *J. Chem. Phys*., Vol. 109, p. 7338, 1998.

14. Murnaghan, F. D*., Proc. Natl. Acad. Sci*. (USA), Vol. 30, p. 244, 1944.

15. Souers, P. C., Forbes, J. W., Fried, L. E., Howard W. M., Anderson, S., Dawson, S., Vitello, P., and Garza, R., ``Detonation Energies from the Cylinder Test and CHEETAH v3.0,", *Propellants, Explosives, Pyrotechnics*, Vol 26, p. 180, 2001.

16. Cohen, S. D. and Hindmarsh, A. C., "CVODE User Guide," Lawrence Livermore National Laboratory Report UCRL-MA-118618, September 1994.

17. Kee, R. J., Ripley, F. M., Meeks, E., and Miller, J. A., "CHEMKIN-III A Fortran Chemical Kinetics Package of the Analysis of Gas-Phase Chemical and Plasma Kinetics," UC-405 SAND96-8216, 1996.

18. Weiser, A. and Zarantonello, S. E., "A Note on Piecewise Linear and Multilinear Table Interpolation in Many Dimensions," *Math. Comp*., Vol. 50, p. 189, 1988.

19. Veldhuizen, T. L., "Grid Filters for Local Nonlinear Image Restoration," Master's thesis, Dept. of Systems Design Engineering, University of Waterloo, May 1998.

20. Joseph Kohler and Rudolf Meyer, *Explosives*, 4th ed. (VCH Press, Weinheim, Germany), p. 260, 1993.

21. D. L. Ornellas, *Calorimetric Determinations of the Heat and Products of Detonation for Explosives: October 1961 to April 1982*, Lawrence Livermore National Laboratory report UCRL-52821 (1982).

22. Don Ornellas, "The Heat and Products of Detonation of TATB", LLNL internal memo, February 10, 1993.

23. F. Volk and F. Schedlbauer, "Analysis of

Post Detonation Products of Different Explosive Charges," *Propellants, Explosives, Pyrotechnics 24*, 182-188 (1999).

24. F. Volk, "Analysis of the Detonation Products of Insensitive High Explosives," *in Advances in Analysis and Detection of Explosives*, J. Yinon, ed (Kluwer Academic Publishers, Netherlands, 1993), pp. 223-239.

25. N. Roy Greiner, D. S. Phillips, J. D. Johnson and Fred Volk, "Diamonds in Detonation Soot," *Nature 333*, 440-442 (1988).

26. V. M. Titov, V. F. Anisichkin and I. Yu. Mal'kov, "Synthesis of Ultradispersed Diamond in Detonation Waves," *Physics Combustion & Explosion (Russian) 25*, 372-379 (1989); English translation.

27. N. V. Kozyrev and E. S. Golubeva, "investigation of the Synthesis of Ultradispersed Diamonds in Mixtures of TNT with RDX, HMX and PETN," *Physics Combustion & Explosion (Russian) 28*, 560-563 (1992); English translation.

28. Souers, P. Clark and R. Garza, private communication, 2006.